Chapter 3

Thermal Residual Stresses

3.1 Grinding Temperature

To study thermal residual stresses, the grinding-induced temperature field needs to be investigated carefully in relation to grinding conditions. For a short workpiece, grinding temperature varies the transient state since more time or a longer moving distance of the input heat flux is required. A typical surface temperature history under different table speeds of grinding is shown in Fig. 3.1.

The grinding temperature ahead of the heat source develops much faster than that behind it as more time is required for thermal energy to diffuse through the workpiece. Moreover, the grinding temperature history approaches its steady state much faster if the Peclet number is higher. Theoretically, the time required to achieve steady conditions is very long. Steady state conditions are reached only when the grinding temperature profile relative to the heat source movement becomes unchangeable. Figure 3.2 exhibits the maximum grinding temperature history in terms of non-dimensional time, $\bar{t}$. It shows that for a given grinding condition (e.g. Pe=1, H=0), $\bar{t}$ should exceed 4 if more than 95 % of the grinding temperature needs to be attained The type of grinding mechanism, i.e. up- or down-grinding, expressed by a different heat flux apex profile, l_a, has little influence on the maximum grinding temperature history. In steady state grinding, the temperature field within the ground component can be explored by considering the iso-curves of the grinding temperature (see Fig. 3.3), which are sets of curves with their centres being coincident with the location of the maximum temperature at the ground surface.

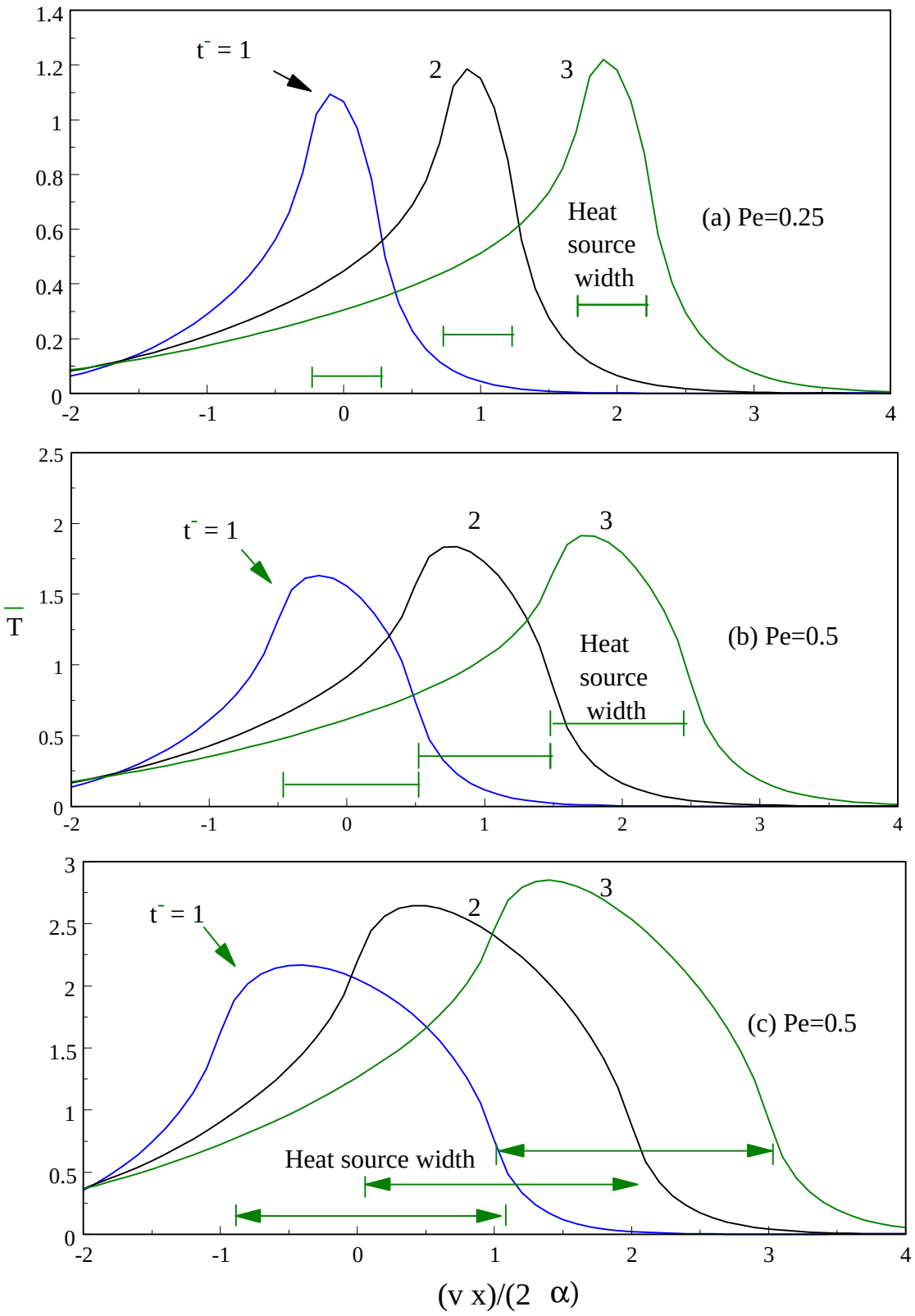

Figure 3.1 Transient surface (H=0)

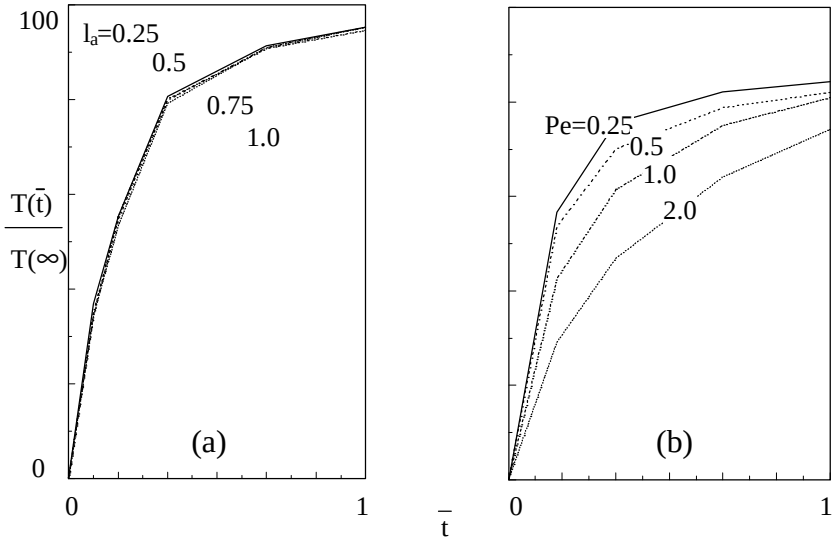

Figure 3.2 Maximum temperature history at the surface of grinding
(a) effect of heat flux profile (Pe=1), (b) effect of Peclet number (l_a

If the convection heat transfer coefficient, H, increases, grinding temperature decreases particularly at the trailing edge of the input heat source. In all cases the maximum grinding temperature is close to the centre of the grinding zone.

3.2 Onset of Thermal Plastic Deformation

One of the major causes of residual stresses in a ground component is thermal-plastic deformation. Under steady state grinding conditions, the effect of the grinding temperature on the maximum effective stress is considered. Figures 3.4 and 3.5 show the relationship between the surface temperature and the effective stress, σ_e. It is apparent that the effective stress distribution is nearly proportional to the grinding temperature across the ground surface. Another similar proportionality is detected across the grinding depth as shown in Fig. 3.5. According to workmaterial properties, the critical maximum grinding temperature for plastic

deformation to take place is 250 ^{o}C as the maximum effective stress equals workmaterial yield stress, Y.

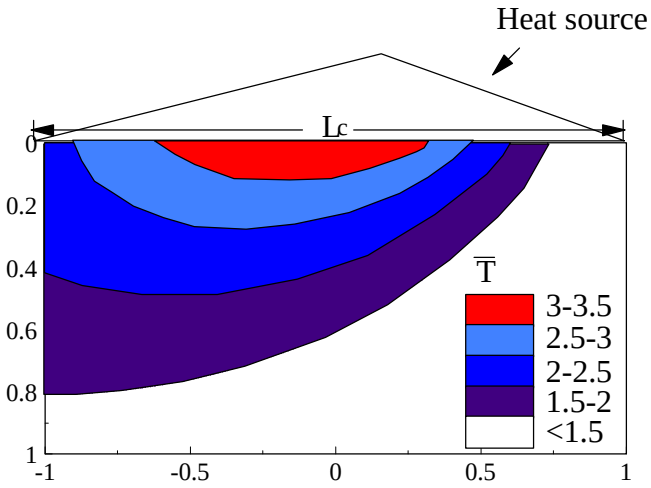

(a) H=0

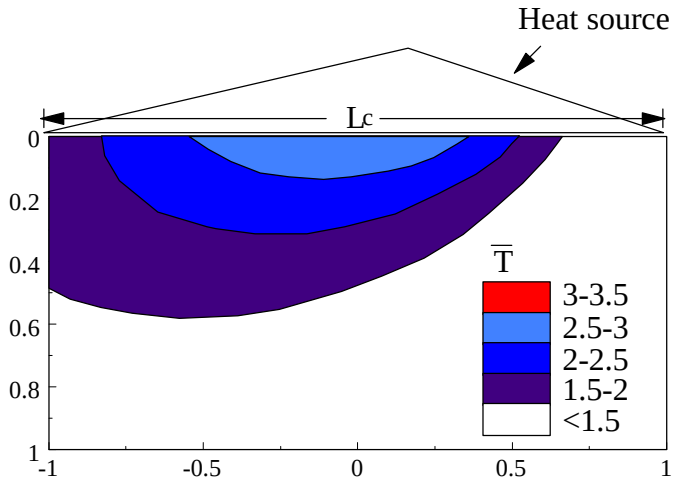

(b) H=0.25

Figure 3.3 Dimensionless temperature field at steady state

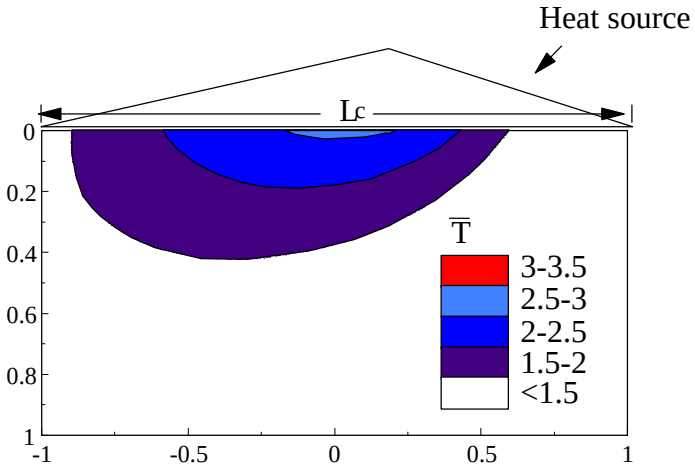

(c) H=0.5

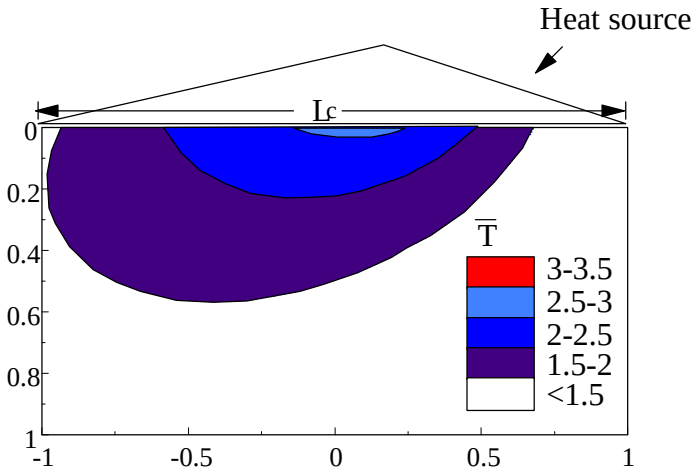

(d) H=1.0

Figure 3.3 Dimensionless temperature field at steady state (continued)

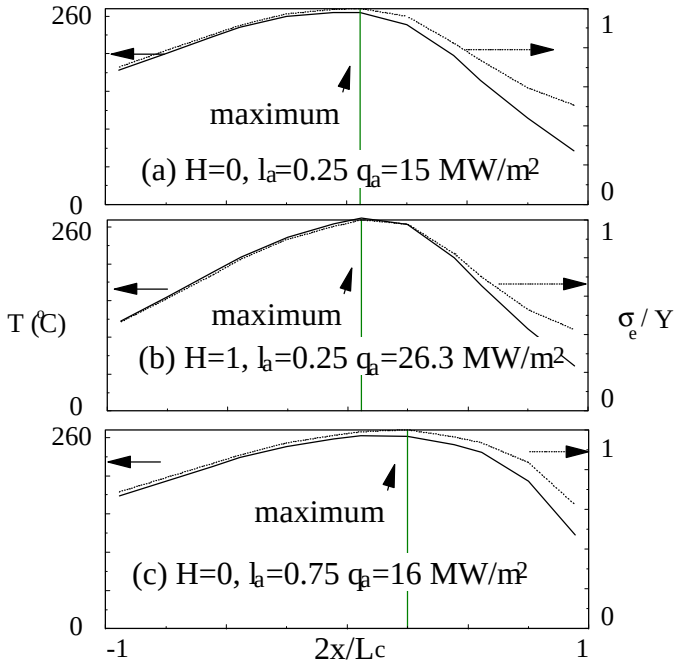

Figure 3.4 Onset of thermal-plastic deformation in relation grinding conditions (Pe=1): a view over the workpiece

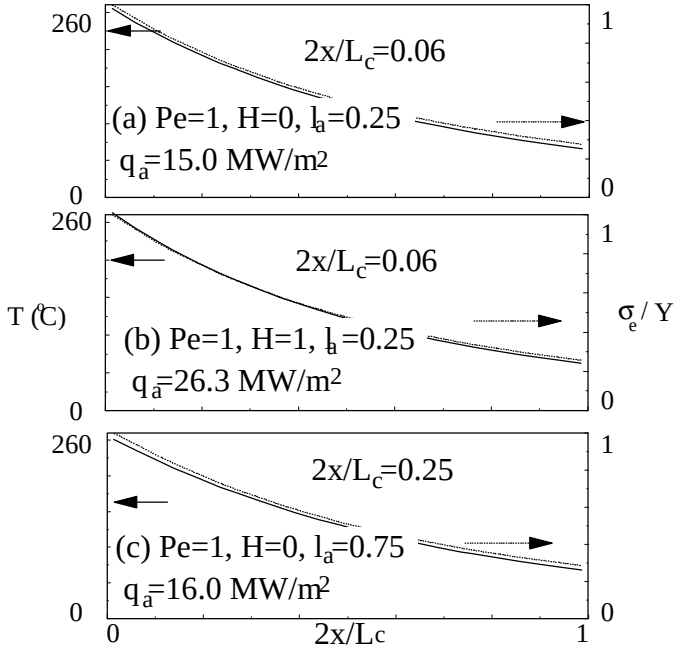

Figure 3.5 Onset of thermal-plastic deformation in relation grinding conditions (Pe=1): a view in the subsurface of workpiece

The stress field within a semi-infinite elastic domain can be regarded as the superposition of mechanical, σ_{me} and thermal, σ_{th} components. By recalling eq. (2.2), the total effective stress can be written as

$$s_e = (0.5\,[(s_1-s_2)^2+(s_1-s_3)^2+(s_2-s_3)^2]\,)^{1/2} \qquad 3.1$$

Under pure thermal loading conditions and plane strain conditions [Boley and Weiner (1960)], the stress components in x-z plane, (i.e. σ_{xx} and σ_{zz}) vanish if temperature variation is linear. In Figs 3.4 and 3.5 a good approximation of temperature linear variation is observed across depth and surface particularly for grinding domain behind the maximum grinding temperature location.

$$s_{yy} = -aET \qquad 3.2$$

Substitution of eq. (3.2) into eq. (3.1) yields

$$s_e = aET \qquad 3.3$$

where a is the mean thermal coefficient of expansion, E is the Young modulus and T is the grinding temperature.

At yielding, the maximum effective stress should be equal to the yield stress, Y. Therefore the maximum grinding temperature at the onset of yielding is

$$T_{max} = Y/(aE) \qquad 3.4$$

By substitution of the properties of EN23 steel provided in Table 2, it is found that the maximum temperature is 256^o C. This means that the onset of the yielding of the workpiece occurs if the maximum grinding temperature reaches 256 ^{o}C. It is in agreement with the FEM prediction of 250^o C. Hence the numerical solution accuracy is acceptable. Furthermore the maximum grinding temperature is a power function of the Peclet number, Pe, as shown in Fig. 3.6.

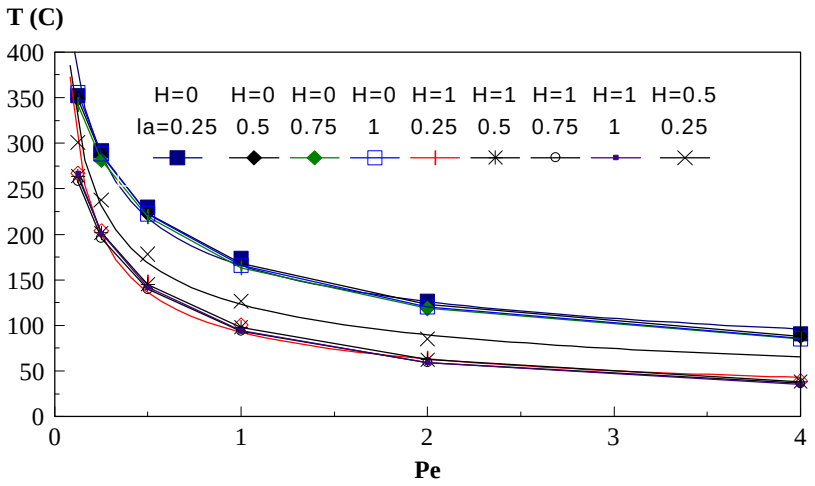

Figure 3.6 Variation of maximum grinding temperature with Pe, H and l_a, (q_a=10 MW/m^2)

Since the grinding temperature is directly proportional to the input heat flux, q_a, it is also useful to express the critical grinding conditions directly in terms of q_a as shown in Fig. 3.7. Fig. 3.7 illustrates that thermal plastic deformation may appear if the input heat flux, q_a, is above the q_a-Pe curves. More input heat flux is needed to initiate plastic deformation as the convection heat transfer coefficient, H, is high. It should be noted that the critical onset curves are affected only slightly by the peak location of an input heat flux profile, l_a. Therefore the cooling power is a more dominant factor for residual stress initiation than the type of grinding mechanism.

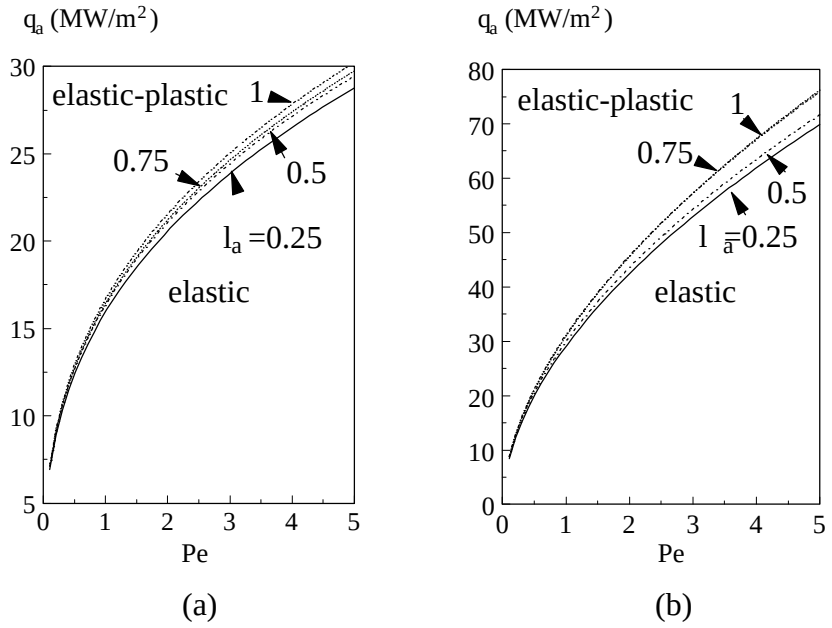

Figure 3.7 Onset of thermal plastic deformation and its variation with Pecklet number (a) H=0, (b) H=1

3.3 Thermal Residual Stresses

3.3.1 Mechanism

The mechanisms of thermal residual stresses can be best understood if the grinding stresses and strains are studied in relation to grinding temperature. The history of the longitudinal thermal strain, $(\varepsilon_{xx})_T$, is traced in Fig. 3.8. It is noted that longitudinal compressive strains start to develop first followed by surface stretching which in turn results in permanent surface strain. To reveal the link between surface thermal stresses and grinding temperature, the stress history associated with the grinding temperature is examined in Fig. 3.9. Figures 3.8 and 3.9 show that the ground components are compressed as grinding temperature rises. This results in both compressive longitudinal and plane stresses, σ_{xx} and σ_{yy} respectively. When the heat source moves away, the grinding temperature cools down therefore the workmaterial tends to contract back to its original shape. However, the irreversible plastic deformation prevents the geometric recovery of the workmaterial and hence tensile residual stresses are

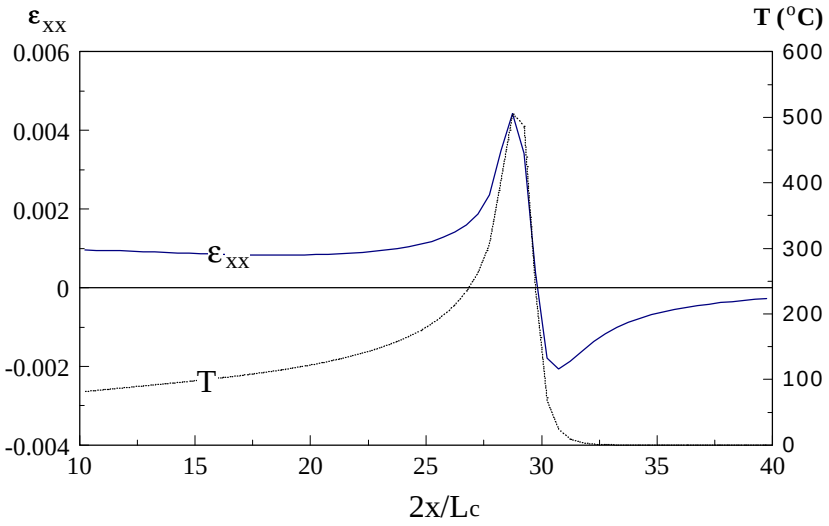

Figure 3.8 Surface longitudinal strain and grinding temperature (q_a=30 MW/m^2, Pe=1,H=0, l_a=0.25)

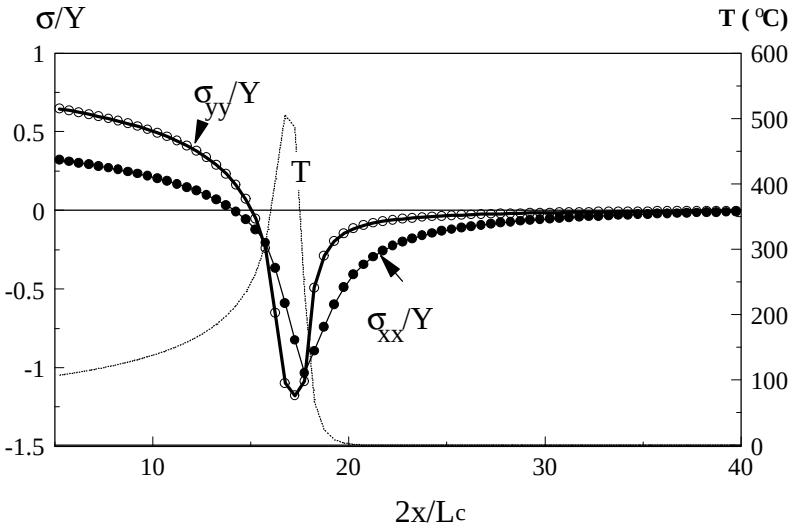

Figure 3.9 Surface stress and grinding temperature q_a=30 MW/m^2, Pe=1,H=0, l_a=0.25

developed. In deeper subsurface layers of the ground component, similar residual stresses are determined but with a change of their nature from tensile to compressive as depth increases (see Fig. 3.10) .

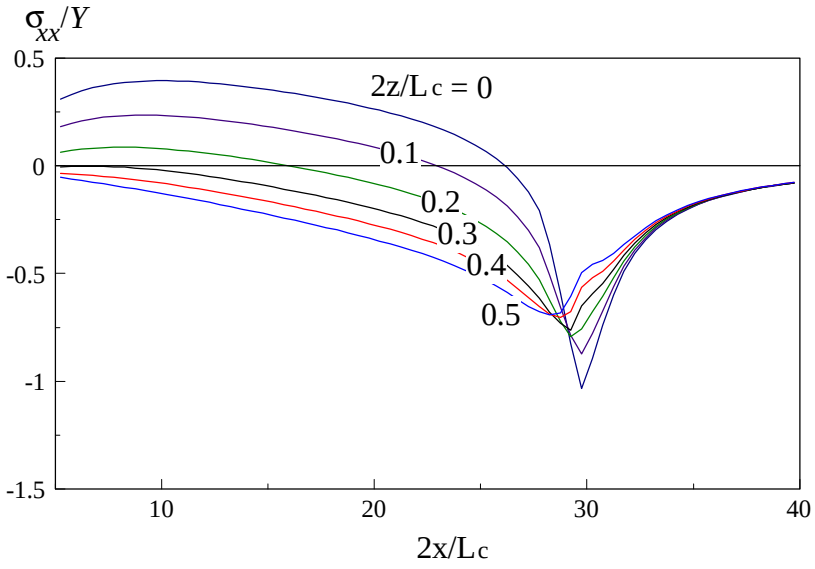

(a) longitudinal stress, σ_{xx}

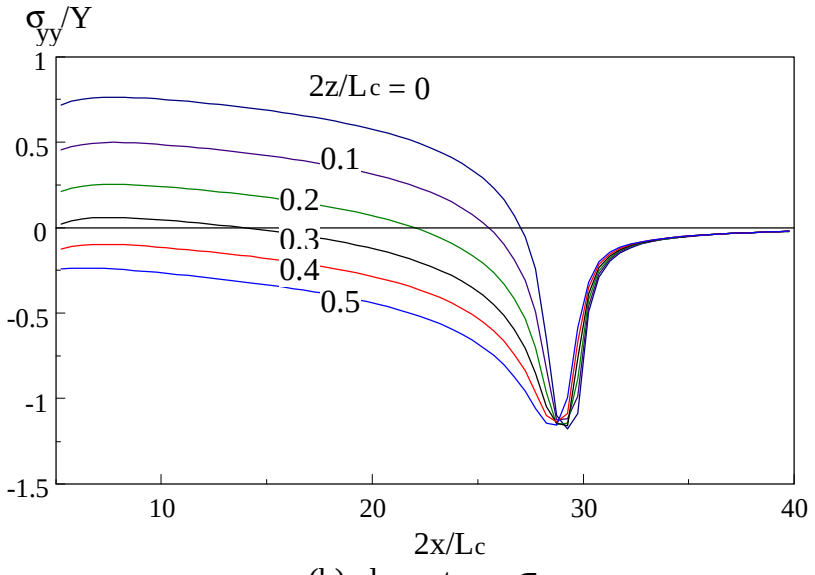

(b) plane stress, σ_{yy}

Figure 3.10 Stress history vs depth
(q_a =30 MW/m2, Pe=1, H=0, l_a =0.25)

A closer understanding of residual stress development can be fulfilled by monitoring the plastic zone development associated with heat source movement as shown in Fig. 3.11. With a

lower heat flux intensity (Fig. 3.11a), the plastic zone is developed in the vicinity of the ground surface. At a higher heat flux intensity (see Fig. 3.11b), however, another plastic zone is developed at the trailing edge of the workpiece. This is attributed to the higher thermal stresses developed as the grinding temperature is higher under a higher heat flux intensity, q_a. When q_a varies, the depth of the residual plastic zone also changes as illustrated in Fig. 3.12. It shows that a permanent plastic zone starts to build up if the heat flux intensity, q_a, is beyond 30 MW/m^2. The depth of the plastic zone increases as heat flux intensity rises. Below a critical heat flux intensity, the workpiece can be free from thermal residual stresses.

3.3.2 Reliability

For a reliable study of grinding thermal residual stresses, a study with an adequate control volume and solution steps needs to be conducted in order to maintain close steady state conditions. Here the surface effective stress history is traced in relation to solution steps. Figure 3.13 demonstrates the role of the number of solution steps in computed residual stresses. It indicates that 136 solution steps are reasonable as a further increase of solution steps has no effect on stresses.

Figure 3.13 also shows that the surface stress profile reaches its steady state not far away from the left edge of the ground workpiece, x=0. Thus the length of the control volume should be suitable for further residual stress computations. To confirm the validity of this control volume, the grinding stresses are evaluated with different levels of input heat flux as indicated by Fig. 3.14. It is clear that steady state conditions can be accomplished shortly regardless of the level of the input heat flux, q_a. The effective stress history indicates that a rapid rise of stress level starts immediately after the heat source movements for all levels of heat flux intensities. Steady state conditions start after a movement corresponds to $2x/L_c=5$. Therefore to obtain reliable residual stresses associated with steady state grinding conditions at different horizontal locations in the workpiece, examination at a section of $2x/L_c$ 5 is

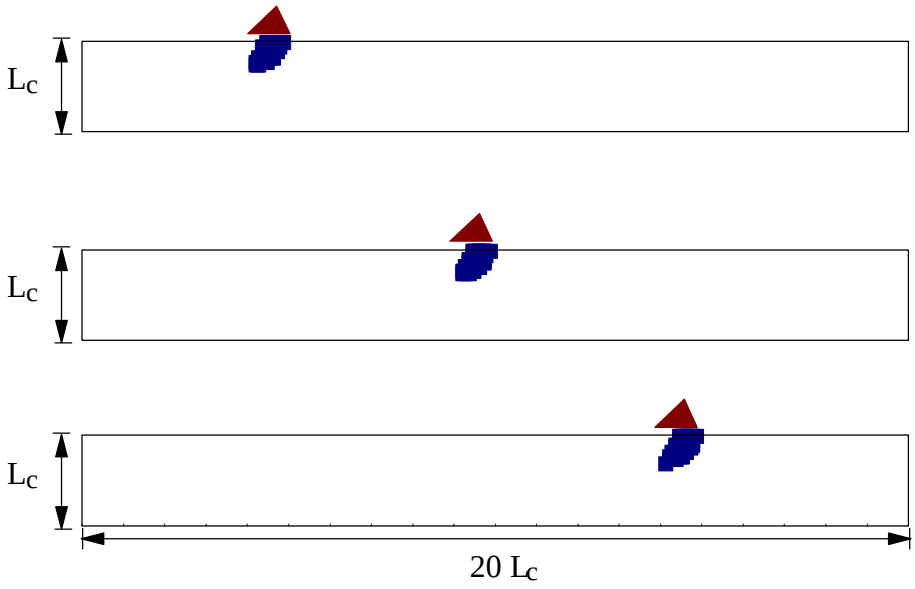

(a) q_a=30 MW/m^2

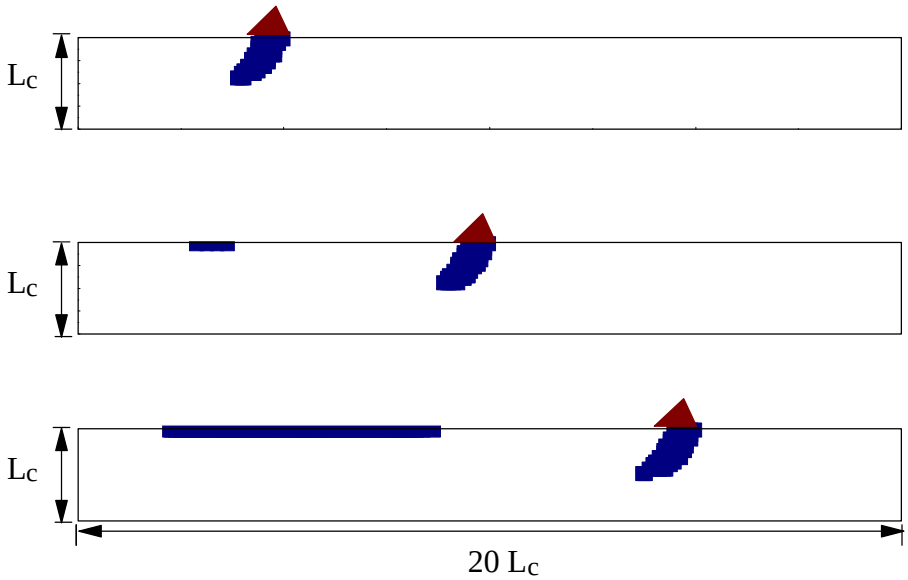

(b) q_a=40 MW/m^2

Figure 3.11 Plastic zone development *vs* heat source location (Pe=1, H=0, l_a =0.25)

necessary. Figure 3.15 shows that there is a slight change of residual stress distributions detected if the section of scanning varies. For the sake of numerical accuracy a location at $2x/L_c$=10.75 will be used, which is the most reasonable scanning section of residual stresses.

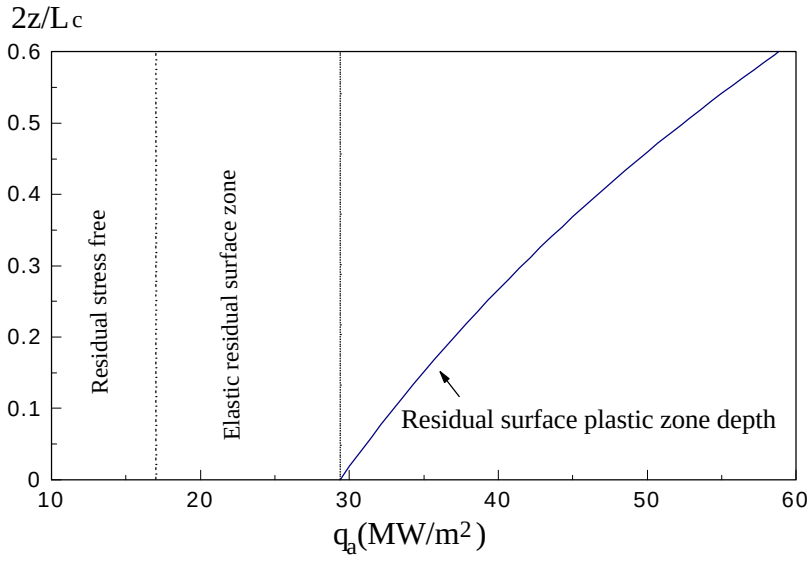

Figure 3.12 Surface plastic zone depth (Pe=1, H=0, l_a =0.25)

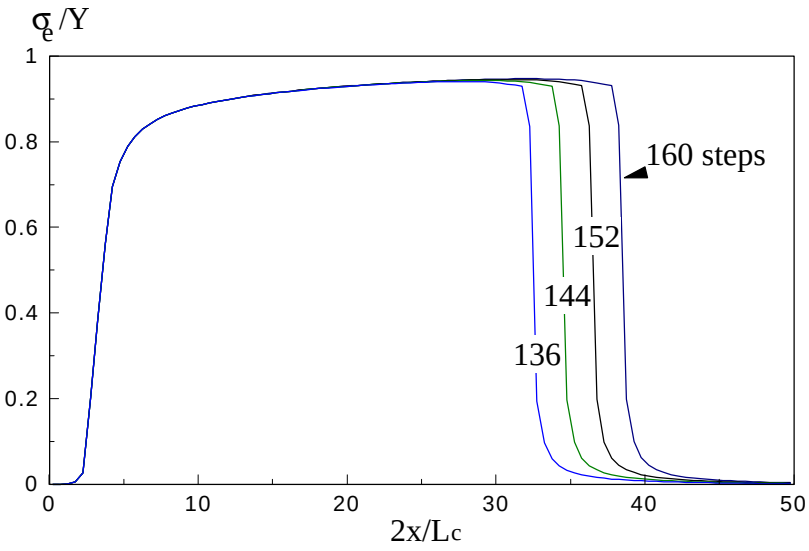

Figure 3.13 Surface thermal residual stresss and number of solution steps (q_a=30 MW/m2, Pe=1, H=0, l_a=0.25)

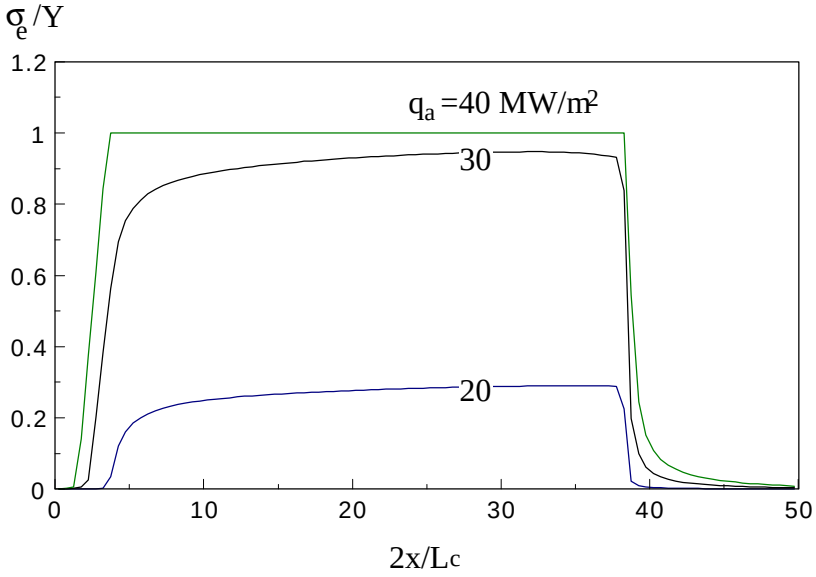

Figure 3.14 Surface thermal residual stress and effect of heat flux intensity , q_a (Pe=1, H=0, l_a=0.25)

3.3.3 Effect of Grinding Conditions on Thermal Residual Stresses

Figure 3.16 shows that grinding type (indicated by peak flux relative location, l_a) has a minor effect on residual stresses. To decrease the level of thermal residual stresses the grinding temperature should be lowered by either enhancing the cooling power of the cooling fluid or by increasing the table speed with all other conditions maintained the same. The influence of cooling fluid (H=1) is shown in Fig. 3.16e which indicates the magnificent effect of convection heat transfer on the residual stress distribution. This is because cooling decreases the thermal residual stresses if heat flux intensity is kept the same as in Fig. 3.16a. However, with a more powerful cooling, the residual stresses variation with depth becomes much steeper.

Another way to decrease the grinding temperature is by enlarging the table speed reflected by the Peclet number, Pe (see Fig. 3.16f). It is apparent that a higher table speed has a greater role in decreasing the thermal residual stresses if heat flux intensity is maintained constant. However, the cooling fluid has a greater effect than table speed in reducing the level of residual stresses. The heat energy transferred by cooling fluid is strongly dependent on the

grinding conditions. Therefore it is sometimes more advantageous to apply a higher table speed if grinding power is maintained unchanged. Figure 3.17 examines the influence of heat flux intensity on surface residual stresses. It shows that the surface residual stress is dependent on low levels of heat flux intensities. For a higher heat flux intensity the residual stresses are no longer affected (to a limit) and become nearly constant. This is directly related to the non-workhardening characteristics with a constant workmaterial yield stress, Y. However, grinding type (the peak location, l_a), i.e. up- or down grinding, certainly has influence on the surface residual stresses.

3.4 Summary

In this chapter, the development of thermal residual stresses in relation to thermal grinding conditions was investigated in detail. Accordingly, the onset of thermal plastic deformation was explored and a set of critical conditions was identified. The mechanism of residual stresses, the reliability of thermal stress modelling and the effect of thermal grinding conditions on residual stresses were fully understood.

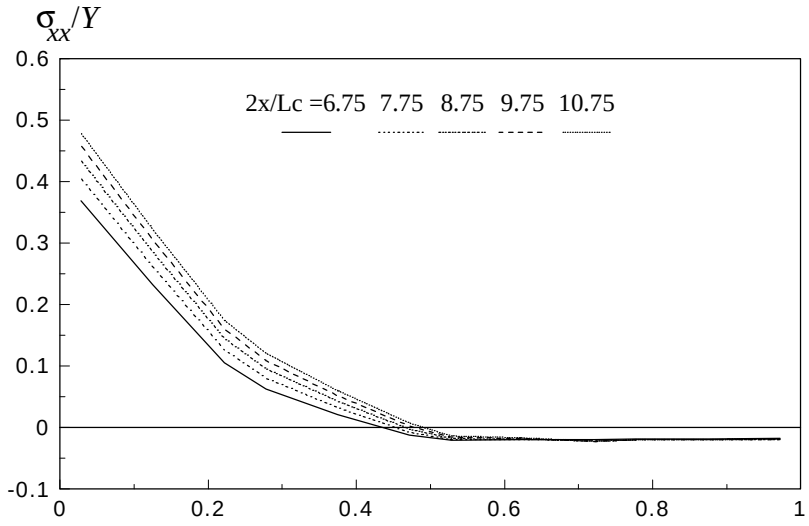

(a) logitudinal stress

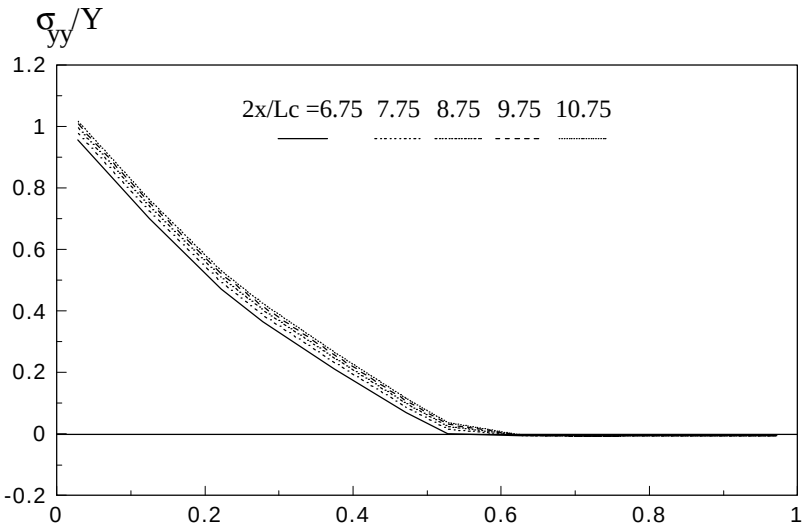

(b) plane stress

Figure 3.15 Residual stress and x-location
(q_a=30 MW/m², Pe=1, H=0, l_a =0.25)

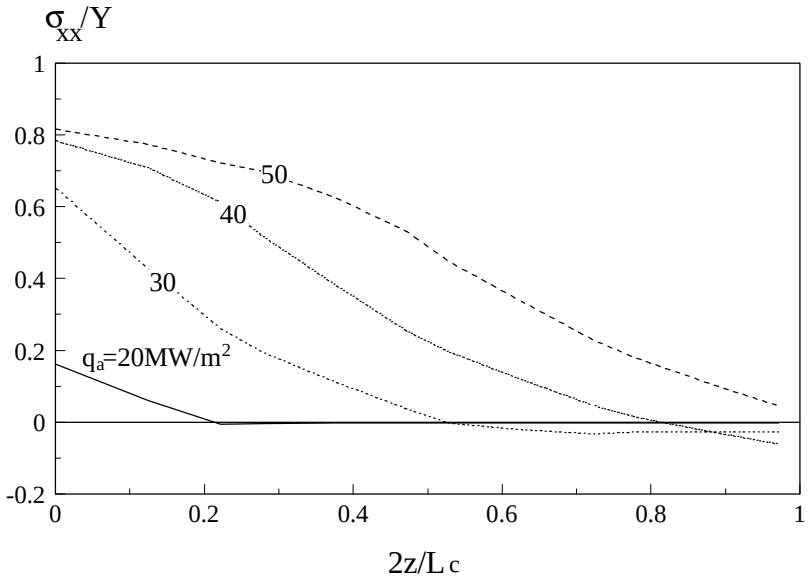

(a) longitudinal stress , l_a=0.25 (Pe=1, H=0)

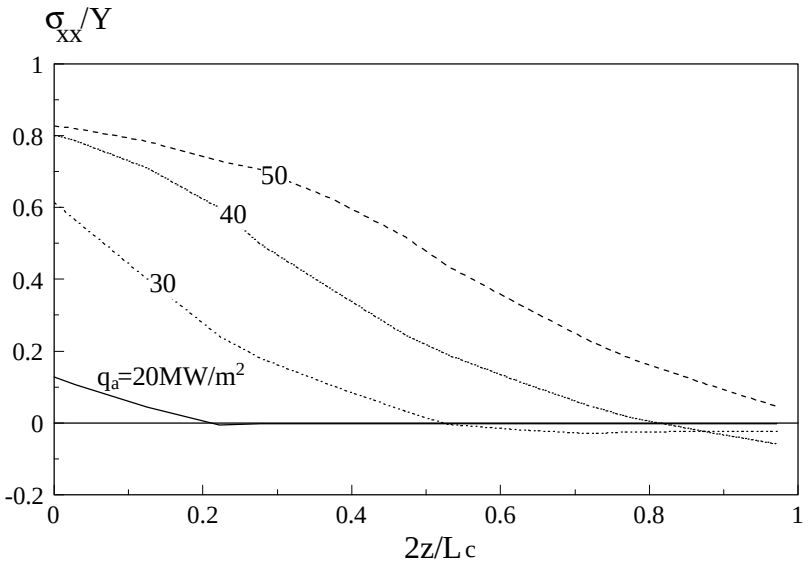

(b) longitudinal stress , l_a=0.75 (Pe=1, H=0)

Figure 3.16 Thermal residual stresses vs heat flux intensity, q_a

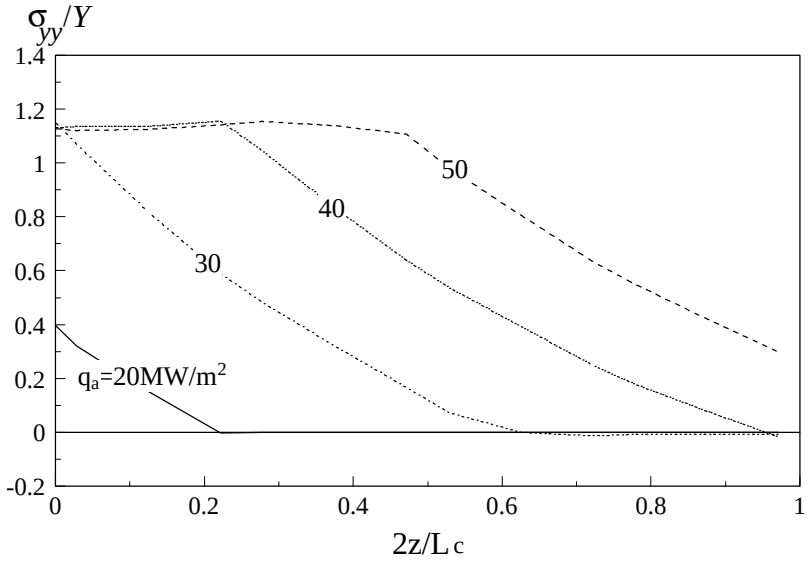

(c) plane stress , l_a=0.25 (Pe=1, H=0)

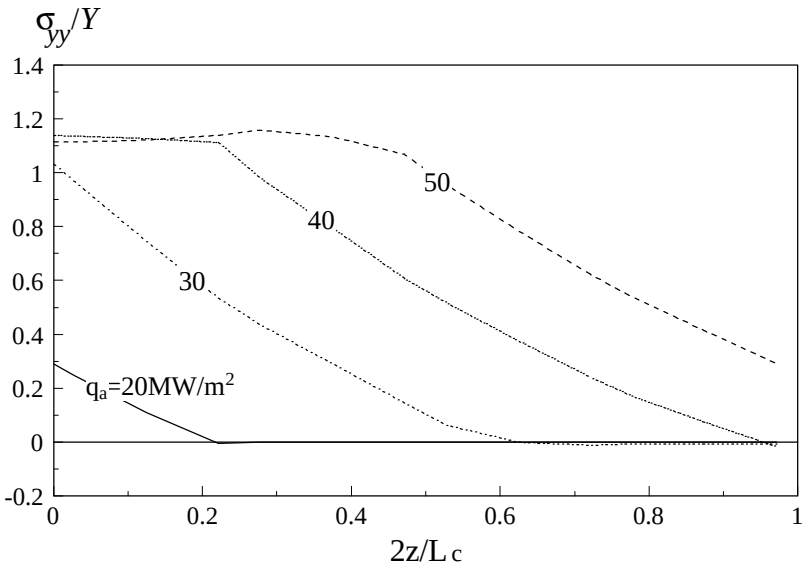

(d) plane stress , l_a=0.75 (Pe=1, H=0)

Figure 3.16 Thermal residual stresses vs heat flux intensity, q_a (continued)

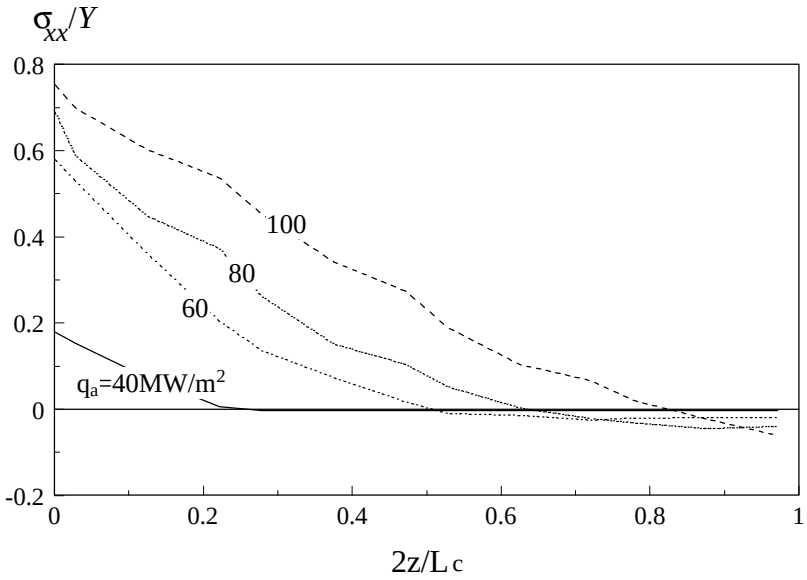

(e) longitudinal stress , l_a=0.25 (Pe=1, H=1)

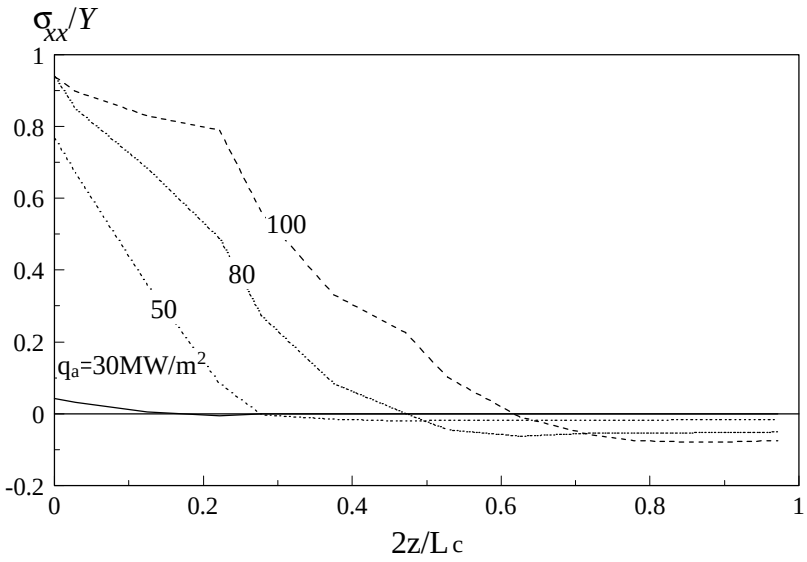

(f) longitudinal stress , l_a=0.25 (Pe=4, H=0)

Figure 3.16 Thermal residual stresses vs heat flux intensity, q_a (continued)

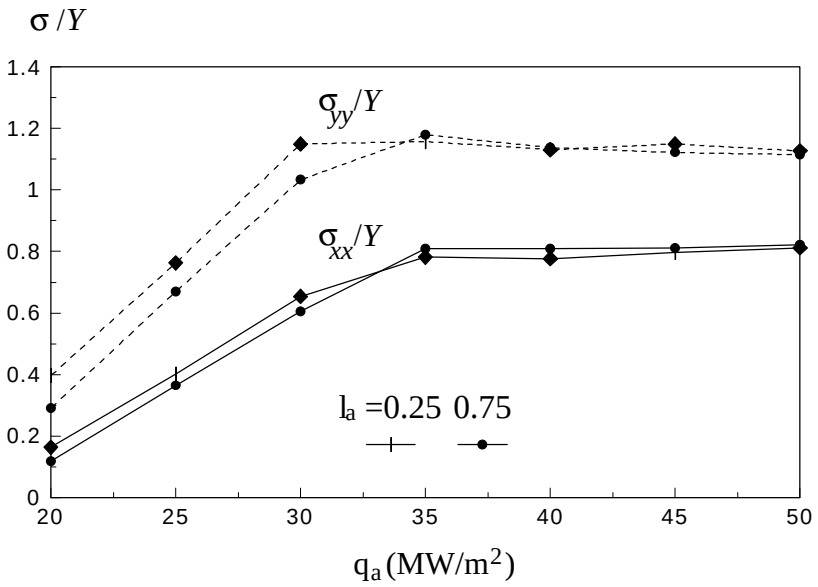

Figure 3.17 Surface thermal residual stresses *vs* heat flux intensity, q_a (Pe=1, H= 0)